

Article

Morphometric Analyses of Phenotypic Plasticity in Habitat Use in Two Caspian Sea Mulletts

Shima Bakhshalizadeh ^{1,*}, Keyvan Abbasi ², Adeleh Rostamzadeh Liafuie ³, Ali Bani ^{1,4}, Anu Pavithran ⁵ and Francesco Tiralongo ^{6,7,*}

¹ Department of Marine Science, Caspian Sea Basin Research Center, University of Guilan, Rasht 4199613776, Iran

² Inland Waters Aquaculture Research Center, Iranian Fisheries Sciences Research Institute, Agricultural Research, Education and Extension Organization, Bandar Anzali 43, Iran

³ Faculty of Natural Resources, University of Tehran, Karaj 31587-77871, Iran

⁴ Department of Biology, Faculty of Science, University of Guilan, Namjo Street, Rasht 41335-1914, Iran

⁵ Independent Researcher, Bangalore 560012, India

⁶ Department of Biological, Geological and Environmental Sciences, University of Catania, 95124 Catania, Italy

⁷ Ente Fauna Marina Mediterranea—Research Organization for Protection and Conservation of Marine Biodiversity, 96012 Avola, Italy

* Correspondence: sh.bakhshalizadeh@guilan.ac.ir (S.B.); francesco.tiralongo@unict.it (F.T.);

Tel./Fax: +98-13-3369-1066 (S.B.)

Abstract: To understand the functional meaning of morphological traits in the exploitation of natural resources, it is necessary to develop a quantitative, meaningful scheme for understanding ecophenotypes; this will facilitate management and conservation, which are the most pressing challenges in vulnerable aquatic environments. In this context, the management of cryptic and very similar species is more challenging, because of the difficulty of distinguishing them and determining their frequency in sympatry, even though they do not necessarily have the same ecologies. As such, in order to understand how morphological similarities are associated with their ecology, thirteen morphometric characteristics related to body landmark-based geometric morphometries, sagittal otolith morphology, and shape were examined in mature *Chelon auratus* and *Chelon saliens*, which were collected from the coastal waters of the southwest Caspian Sea between October 2020 and April 2021. Univariate and multivariate analysis of variance were conducted to evaluate the potential morphological differences between the species. The analyses highlight the morphological differences between *C. auratus* and *C. saliens*, and identify potentially helpful traits for using body and otolith shape for the interspecific distinction of these very similar species of Caspian mullet, which can reflect functional similarity and are an important component of community ecology.

Keywords: Mugilidae; characteristic habitats; limiting similarity; discrimination; species description



Citation: Bakhshalizadeh, S.; Abbasi, K.; Rostamzadeh Liafuie, A.; Bani, A.; Pavithran, A.; Tiralongo, F. Morphometric Analyses of Phenotypic Plasticity in Habitat Use in Two Caspian Sea Mulletts. *J. Mar. Sci. Eng.* **2022**, *10*, 1398. <https://doi.org/10.3390/jmse10101398>

Academic Editor: Dariusz Kucharczyk

Received: 8 August 2022

Accepted: 21 September 2022

Published: 30 September 2022

Publisher's Note: MDPI stays neutral with regard to jurisdictional claims in published maps and institutional affiliations.



Copyright: © 2022 by the authors. Licensee MDPI, Basel, Switzerland. This article is an open access article distributed under the terms and conditions of the Creative Commons Attribution (CC BY) license (<https://creativecommons.org/licenses/by/4.0/>).

1. Introduction

Understanding how morphological characteristics change among species with different ecological habits aids our efforts to conserve and manage natural resources, and improves our limited knowledge of the ecology of many living species in the aquatic environments, even in overexploited habitats [1–4]. In addition to feeding habits, a variety of ecological attributes, such as substrate use, and environmental factors including salinity, dissolved oxygen, current flow, temperature, and water depth, is generally related to variations in morphology [5,6]. Although the ecophenotype is associated with phylogenetic relatedness, common adaptive responses and the contingent behaviors remain understudied; knowledge of these factors is fundamental for organizing strategies to preserve and sustain biological diversity [7–11]. However, this task is particularly challenging for cryptic and extremely similar species which hardly differ based on external morphology alone,

and which therefore require a unified approach that uses both body morphology and otolith morphology tools [1,12]. Meanwhile, intentionally introducing species to a new habitat is a global practice that changes the biological outlook, due to factors including the success probability of these newcomers and also their influence on the niche space within the recipient community [13–16]. In our study, we analyzed two similar species of the family Mugilidae: *Chelon auratus* (Risso, 1810) and *Chelon saliens* (Risso, 1810). These species were successfully introduced to the Caspian Sea and have been regarded as naturalized in the Caspian Sea waters from the latter half of the 1960s [13,17]. The mullets are broadly distributed in the south Caspian Sea, and migrate to coastal zones during autumn to overwinter, consequently increasing their catch. They are one of the major commercial species in the south Caspian Sea, and are consumed canned, smoked, or fresh, and are used as bait for birds such as Great Cormorant, *Phalacrocorax carbo* [13,18–20]. Both species are characterized by a compressed and subcylindrical body, with a slightly dorsoventrally flattened head [13,17].

Chelon saliens is an inshore pelagic species generally found in Mediterranean estuaries and in the northeast Atlantic at salinities of 4–13‰. In the southern Caspian, the species migrates to waters with temperature and salinity levels ranging from 5–27 °C and 11–28‰, respectively. However, fry need time to adapt to lower salinities [13,21]. Their diet is similar to that of *C. auratus*, comprising periphyton, detritus, and small benthic organisms, as well as sand grains contained in the stomach [13]. Adults feed on algae and detritus, while juveniles feed on zooplankton and benthic organisms. Reproduction takes place in summer, and eggs are pelagic. Adults are usually found in schools in coastal waters, and sometimes in estuaries and lagoons; meanwhile, juveniles are mainly confined to coastal lagoons and estuaries during summer and autumn [22].

Chelon auratus shows a similar geographic distribution to *C. saliens*, being confined to the Mediterranean and northeastern Atlantic. Adults are usually found in schools and are neritic, entering coastal lagoons and estuaries in winter and especially in spring, and show a high degree of adaptability to a wide range of salinity levels [13,23]. Juveniles feed on zooplankton only, while adults mainly feed on small benthic organisms and detritus. Reproduction is reported to take place between July and November, and eggs are pelagic [22].

Recently, the catching of mullets was restricted to the study of phenotypic variation, which is necessary for identifying discrete phenotypic populations [24,25]. Phenotypic plasticity is the ability of the observable traits of a genotype to differ in response to different environmental stimuli [26–28]. Investigations into the phenotypic plasticity of fish started in the mid-20th century, and have played an important role in improving our understanding of biological diversity in fish by relating their morphs to their ecological roles [26]. As morphological relatedness is associated with ecological similarity and seems to be a proxy for its ecological role in the ecosystem, understanding the shape differences between closely related species and being able to identify them correctly are fundamental and pressing challenges for management and conservation in modern society [29,30]. The correct identification of such species requires an experienced observer, otherwise many misclassification errors occur [1,12,31]. This paper focuses on two sympatric and very similar species, *C. saliens* and *C. auratus*, to infer the ecophenotype variation underlying the genetic diversity in these species that are dispersed in the morphospace, and which therefore deserve species-specific management strategies. Furthermore, morphological differences can facilitate the coexistence of closely related fish and enhance ecological partitioning between competitors [32]. Our hypothesis is that the two studied species differ in external morphology, and that habitat segregation facilitates their coexistence, since morphology and ecology are often closely related [32] and references therein.

2. Materials and Methods

In total, 72 individual mullets were obtained from commercial fishery catches in the southwest of the Caspian Sea (38°26' N, 49°54' E) taken by beach seine from October

to April 2021 (Figure 1); they were classified as 2 morphological species (*C. auratus* and *C. saliens*) according to the current taxonomic key [13,17]. As all animal handling was conducted under the Iranian and European guidelines on animal welfare, and the waste matter was used for differentiation purposes, no ethical committee approval was necessary, nor were the experiments regulated by laws on animal testing. As no sexual dimorphism is observed in *C. auratus* and *C. saliens*, for each individual, total body weight was measured to the nearest gram, and total length was measured nearest to cm; then, the right sagittal otolith was extracted, cleaned, dried in a dark place, and stored for analysis. The lengths of the collected *C. auratus* (n = 30) ranged from 21.9 to 46.2 cm, and from 21.9 to 31.0 cm for *C. saliens* (n = 42).

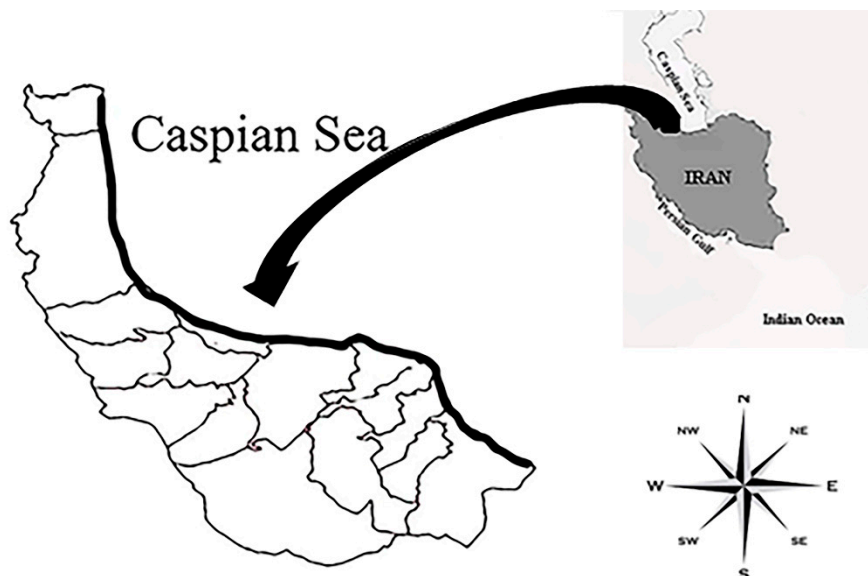


Figure 1. Sampling location of mullet (*Chelon auratus* and *Chelon saliens*) individuals collected in the southwest coastal waters of the Caspian Sea between March 2021 and October 2021.

Photographs of the right sides of each fish were taken using a Sony W270 digital camera, Japan. Overall, 13 landmarks, based on standardized images of the right sides of the individuals, were used to define the point configurations (Figure 2) of the fish body (NBL = 13); NBL = number of fish body landmarks. Analyses were performed using the tps software package (<http://life.bio.sunysb.edu/morph/> accessed on: 7 July 2022). After first concatenating all photographs into a single file, we applied 13 morphological landmarks (Figure 2) that were placed in the tps Dig 2 program [33]. By applying the generalized least-squares procedure, the confounding effects of translation, rotation, and scaling were removed. The centroid size for each specimen and uniform components were obtained using PAST software by Procrustes superimposition for subsequent analysis, according to Zelditch et al. [34]. We followed the methodology of Frassen [35] to remove any inconsistent binding of fish samples owing to rigor mortis [35,36].

High quality otolith images were taken using a binocular microscope from KRUSS co., Germany. After weighting each sagittal otolith to the nearest g, the sagittal otolith was placed against a black background oriented with the sides up, down, and lateral in order to measure OL (Otolith length), OH (Otolith height), and perimeters (P) to the nearest mm. Area (A) to the nearest mm² was measured using ToupView Imaging Software; the method followed Tuset et al. [37] and Bani et al. [38]. Afterwards, shape descriptors such as OH'/OL', rectangularity (A/(OL × OH)), compactness (P²/A), circularity (P²/A), the aspect ratio (OL/OH), roundness (4A/(π (OL)²)), ellipticity ((OL – OH)/(OL + OH)), and form factor (4πA/P²) were estimated.

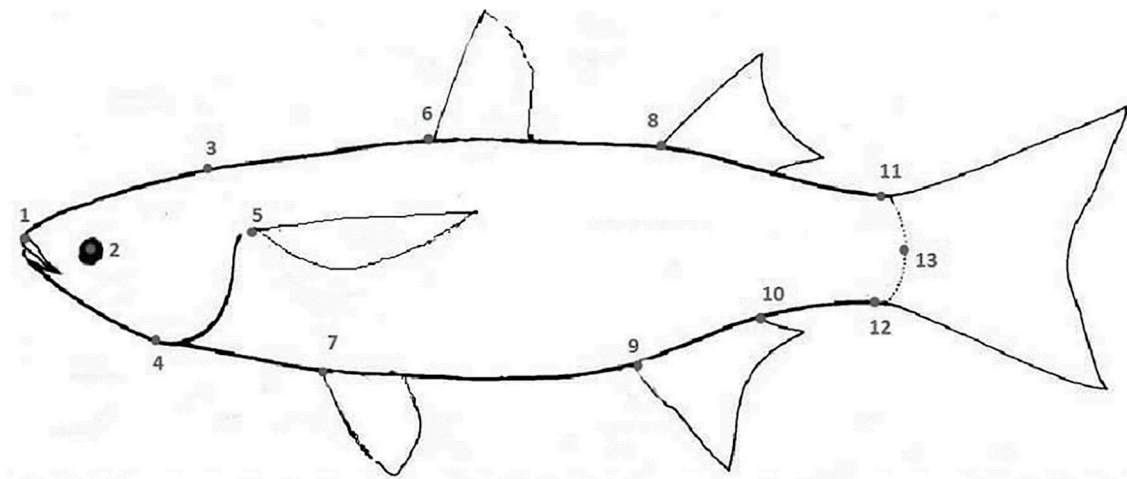


Figure 2. General drawing of the mullet collected in the southwest coastal waters of the Caspian Sea, showing the configuration of 13 landmarks. Landmarks are defined as follows: (1) tip of snout; (2) center of eye; (3) forehead; (4) lower part of operculum; (5) origin of pectoral fin; (6) origin of first dorsal fin; (7) origin of pelvic fin; (8) origin of second dorsal fin; (9) origin of anal fin; (10) ending of anal fin; (11) anterior attachment of dorsal membrane from caudal fin; (12) anterior attachment of ventral membrane from caudal fin; and (13) posterior end of vertebrae column. Inter-landmark distances used for linear morphological traits: caudal peduncle depth (CP):11–12, body depth posterior (BDP): 8–9, body depth anterior (BDA): 6–7, post-pelvic fin length (PPF): 7–13, head depth (HD): 3–4.

All measurements were normalized to standard body size by taking into account the allometric relationships to minimize differences in otolith size [38–40]. The allometric relationship between total length and each otolith measurement was calculated for each species, using the standard equation $y = ax^b$ [40]. Then, logarithmic transformation was applied to homogenize the residuals [38]. Each measure (y) was transformed into z according to $z = y(x_0 \cdot x^{-1})^b$, where x is the original body length of each individual, x_0 is the reference total length, and b is the allometric parameter relating the dependent variable y (each otolith measurement) to the independent variable x (total length) [40].

To detect significant differences between the mean functions of various groups, ANOVA was used to analyze the standardized values of each morphological characteristic as the dependent variable, based on the two species, as the factor. Principal component analysis (PCA) with a correlation matrix was used to visualize the overall differences using the morphometric features. PCA identifies new and meaningful variables based on a combination of the original traits, and reduces many variables to a few principal components (PC). Any component with an eigenvalue greater than one was applied in subsequent analysis. Discriminant analysis was used to analyze the scores of all non-zero principal components (PCs) to identify species-specific variation and group separation based on generalized Mahalanobis distances of ten morphometric features [41]. Stepwise insertion of variables was used to minimize the sum of unexplained variance for all groups [41]. To determine whether this variability could group the species, a cluster analysis was performed using Euclidean distance on the basis of the Ward method.

All statistical analyses were carried out using SPSS (v. 20, Chicago IL, USA) with a level of significance of 0.05. Sigmaplot (Version 2000, Systat software Inc., San Jose, CA, USA) and Excel (Version 2007) were used to plot the data.

3. Results

The geometric morphometric results obtained for the 13 landmarks allowed the clear discrimination of both species. The overall assignment of individuals to their original species was 98.6%, with values ranging from 90% for *C. auratus* to 88% for *C. saliens*.

Most notable were the differences between *C. auratus* and *C. saliens* in terms of the distance between head landmarks and the length of the anal fin (Table 1). *Chelon auratus* exhibited a relatively elongated snout and body, and a bigger head than *C. saliens*, although the caudal peduncle in *C. saliens* was wider than that in *C. auratus* (Table 1). Furthermore, the eyes were in lower part of the head in *C. auratus*, while the distance between the anal fin and caudal fin was smaller in *C. saliens* (Table 1).

Table 1. The ANOVA results for morphometric measurements of the body shapes of two mullet species (*Chelon saliens* and *Chelon auratus*) collected from the south Caspian Sea between March 2021 and October 2021. *p* is considered as being significant if <0.05 (ANOVA); in bold.

Morphometric Measurements	F Value	<i>p</i> Value	Morphometric Measurements	F Value	<i>p</i> Value	Morphometric Measurements	F Value	<i>p</i> Value
1-2	14.92	0.00	3-7	1.01	0.32	6-9	20.73	0.00
1-3	23.39	0.00	3-8	2.66	0.11	6-10	4.89	0.03
1-4	16.19	0.00	3-9	45.38	0.00	6-11	1.69	0.20
1-5	18.50	0.00	3-10	19.78	0.00	6-12	4.12	0.05
1-6	7.84	0.01	3-11	0.70	0.40	6-13	2.77	0.10
1-7	1.62	0.21	3-12	4.16	0.05	7-8	6.01	0.02
1-8	4.71	0.03	3-13	2.46	0.12	7-9	23.13	0.00
1-9	16.67	0.00	4-5	0.20	0.66	7-10	8.65	0.00
1-10	1.20	0.28	4-6	0.82	0.06	7-11	0.00	0.97
1-11	37.66	0.00	4-7	3.30	0.07	7-12	1.81	0.18
1-12	56.88	0.00	4-8	11.00	0.00	7-13	0.85	0.36
1-13	55.90	0.00	4-9	40.82	0.00	8-9	2.12	0.15
2-3	41.68	0.00	4-10	18.30	0.00	8-10	2.16	0.15
2-4	1.21	0.27	4-11	0.92	0.34	8-11	5.12	0.03
2-5	19.55	0.00	4-12	0.00	0.95	8-12	2.33	0.13
2-6	6.81	0.01	4-13	0.04	0.84	8-13	5.51	0.02
2-7	0.26	0.61	5-6	0.28	0.60	9-10	15.74	0.00
2-8	1.64	0.20	5-7	7.73	0.01	9-11	50.81	0.00
2-9	47.42	0.00	5-8	6.29	0.01	9-12	56.42	0.00
2-10	9.29	0.00	5-9	50.50	0.00	9-13	62.21	0.00
2-11	19.33	0.00	5-10	19.58	0.00	10-11	19.02	0.00
2-12	22.34	0.00	5-11	0.00	1.00	10-12	24.35	0.00
2-13	29.79	0.00	5-12	0.81	0.37	10-13	27.38	0.00
3-4	13.75	0.00	5-13	0.58	0.45	11-12	26.94	0.00
3-5	2.15	0.15	6-7	3.17	0.08	11-13	1.24	0.27
3-6	0.27	0.61	6-8	0.59	0.44	12-13	1.68	0.20

Principle component analysis revealed that 75% of the total variation in body morphology was due to the first four components, which explained 47.48%, 12.59%, 7.92%, and 7.01% of the total variation, respectively (Figure 3). The first principal component (PC1) mainly described body elongation. The distance between the snout and eye landmarks and the caudal fin area differed between *C. auratus* and *C. saliens*. There was a significant difference between the landmark of the species that had the largest eigenvalue (>0.8) loaded in PC1(1-11, 1-12, 1-13, 2-11, 2-12, 2-13, 9-11, 9-12, 9-13, 10-11, 10-12, and 10-13 (*p* < 0.05) (Tables 1 and 2). *Chelon auratus* was characterized by a greater distance from the head landmarks to the caudal fin area than *C. saliens*, meaning that the anterior part of the body of *C. auratus* is more elongated than that of *C. saliens*. The head section of the body and the distance from the anal fin to the end of the body showed the most differences, but the position of the dorsal fins differed less (Table 1). Therefore, the best contrast between individuals is achieved by comparing head length traits with posterior body traits. That is to say that, in *C. saliens*, the head was smaller, the base of the anal fin was located closer to the caudal fin, and the width of the caudal peduncle was greater (Figure 3, Table 2).

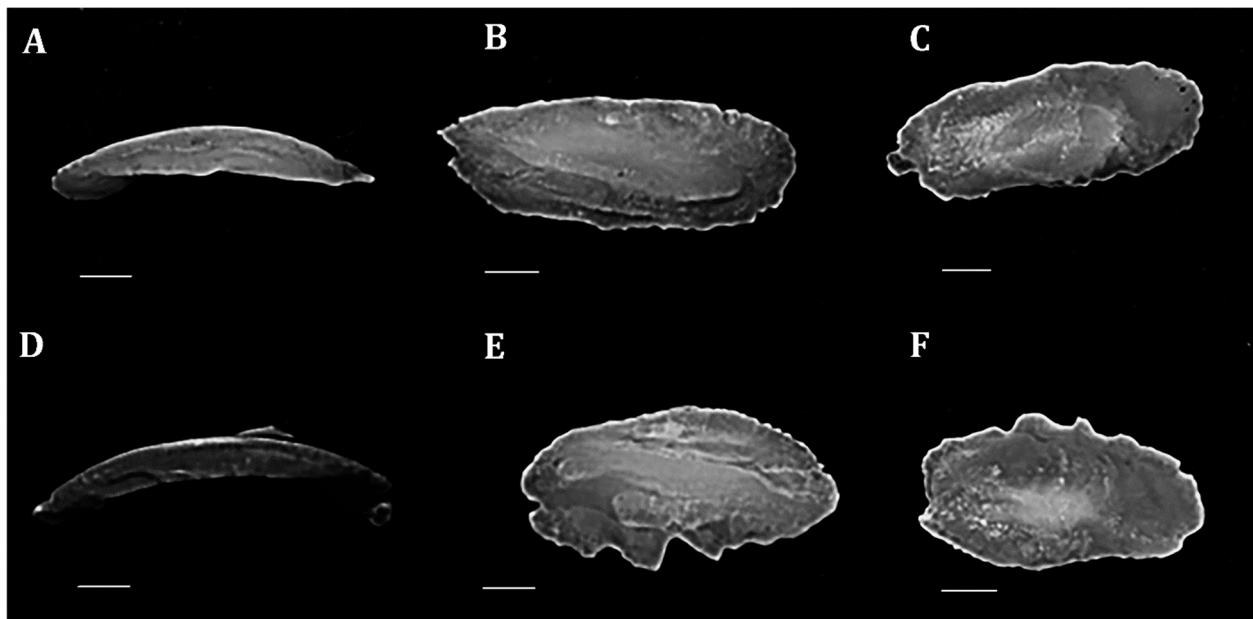


Figure 3. Sagittal otoliths of *C. saliens* (total length, LT = 27.9 cm and otolith length, LO = 7.14 mm): lateral view (A), inside view (B), outside view (C); and *C. auratus* (LT = 31.0 cm and LO = 7.88 mm): lateral view (D), inside view (E), outside view (F). Scale bars = 1 mm.

Table 2. Characteristic loadings for PC1, PC2, PC3, and PC4, resulting from principal components analysis (PCA) of 13 landmarks of the body shape of the mullets (*C. saliens* and *C. auratus*), which together represent a total variance of 75%. Values in bold are significant.

Variable *	Communalities		Component			
	Initial	Extraction	PC1	PC2	PC3	PC4
1-2	1.000	0.829	0.213	0.513	−0.293	0.624
1-3	1.000	0.908	0.494	0.500	0.362	0.026
1-4	1.000	0.972	0.638	0.612	0.089	−0.094
1-5	1.000	0.981	0.509	0.531	−0.252	0.603
1-6	1.000	0.960	0.297	0.744	−0.112	−0.151
1-8	1.000	0.957	0.221	0.827	0.041	0.046
1-9	1.000	0.974	−0.688	0.584	−0.275	0.046
1-11	1.000	0.890	0.843	0.346	−0.081	0.158
1-12	1.000	0.882	0.883	0.249	−0.051	0.067
1-13	1.000	0.870	0.832	0.266	−0.014	0.283
2-3	1.000	0.927	0.639	0.360	0.469	−0.147
2-5	1.000	0.820	0.645	0.387	−0.088	0.417
2-6	1.000	0.942	0.345	0.590	0.075	−0.426
2-9	1.000	0.966	−0.818	0.355	−0.156	−0.210
2-10	1.000	0.967	−0.609	0.309	0.619	0.060
2-11	1.000	0.850	0.849	0.024	0.160	−0.233
2-12	1.000	0.895	0.828	−0.092	0.154	−0.310
2-13	1.000	0.810	0.853	−0.078	0.230	−0.099
3-4	1.000	0.892	0.685	0.439	0.048	−0.199
3-9	1.000	0.955	−0.816	0.251	−0.431	−0.033
3-10	1.000	0.930	−0.752	0.178	0.146	0.254
4-8	1.000	0.946	−0.615	−0.137	−0.132	0.186
4-9	1.000	0.989	−0.906	−0.062	−0.255	0.107
4-10	1.000	0.989	−0.830	−0.161	0.177	0.327
5-7	1.000	0.867	−0.143	−0.060	−0.135	−0.399
5-8	1.000	0.915	−0.368	0.196	0.338	−0.660
5-9	1.000	0.970	−0.900	0.083	−0.078	−0.310
5-10	1.000	0.976	−0.790	−0.007	0.507	−0.161

Table 2. Cont.

Variable *	Communalities		Component			
	Initial	Extraction	PC1	PC2	PC3	PC4
6-9	1.000	0.930	−0.704	−0.080	−0.154	0.189
6-10	1.000	0.967	−0.497	−0.260	0.464	0.432
7-8	1.000	0.893	−0.373	0.037	0.151	−0.166
7-9	1.000	0.990	−0.789	0.059	−0.041	−0.015
7-10	1.000	0.982	−0.681	−0.015	0.413	0.168
8-11	1.000	0.940	0.544	−0.532	−0.122	0.081
8-13	1.000	0.906	0.527	−0.597	−0.074	0.151
9-10	1.000	0.945	0.358	−0.111	0.784	0.366
9-11	1.000	0.930	0.914	−0.253	0.132	0.063
9-12	1.000	0.960	0.914	−0.287	0.165	0.019
9-13	1.000	0.969	0.901	−0.292	0.176	0.131
10-11	1.000	0.954	0.823	−0.230	−0.362	−0.182
10-12	1.000	0.967	0.850	−0.261	−0.318	−0.204
10-13	1.000	0.947	0.840	−0.271	−0.321	−0.087
11-12	1.000	0.427	−0.339	0.091	−0.272	−0.099

* The configuration of 13 landmarks. Landmarks are defined as follows: (1) Tip of snout; (2) center of eye; (3) forehead; (4) end of operculum; (5) origin of pectoral fin; (6) origin of first dorsal fin (7) origin of pelvic fin; (8) origin of second dorsal fin; (9) origin of anal fin; (10) ending of anal fin; (11) anterior attachment of dorsal membrane from caudal fin; (12) anterior attachment of ventral membrane from caudal fin; and (13) posterior end of vertebrae column.

Differences in the morphological characteristics of the bodies of *C. auratus* and *C. saliens* were primarily described by one function. This function separates the two species by explaining 100% of the variation in body shape. The cross-validated classification in the discriminate analysis indicate that 96.7% of all *C. auratus*, and 100% all *C. saliens*, were assigned to the correct provenance. The differences in the morphology of body shape were significant (Wilk’s lambda = 0.16, $\chi^2 = 108.66$, d.f. = 23, $p < 0.05$).

With the exception of otolith weight and length, area, perimeters, compactness, form factor, and circularity, all other morphological variables were significantly different ($p < 0.001$) between the two species (Table 3). The morphological variables of otolith height, OH/OL, and roundness were bigger in *C. auratus* in comparison with *C. saliens*, whereas aspect ratio, rectangularity, and ellipticity were bigger in *C. saliens* (Table 3). For the otolith analyses, PCA reduced the otolith dimensions to three components (PC1 = 35.95%, PC2 = 22.53% and PC3 = 19.59%) (Figure 4, Table 4) and indicated that 78.06% of the total variation in morphological variables was related to the otolith ellipticity, aspect ratio, circularity, compactness, and area (Figure 4, Table 4). The high positive loadings are related to the ellipticity and aspect ratio for PC1, the circularity and compactness for PC2, and the area for PC3, as shown in Table 4. The otoliths of *C. saliens* were elongated, and more rectangular and elliptical than those of *C. auratus*.

Table 3. Morphological variables of the otolith in *C. auratus* and *C. saliens* species found in the southwest of the Caspian Sea. Variables marked with * and in bold are significantly different ($p < 0.05$). (ANOVA).

Morphological Variables +	Mean ± SE		p Value
	<i>Chelon auratus</i>	<i>Chelon saliens</i>	
Otolith weight (OW) (g)	0.03858 ± 0	0.03887 ± 0	0.899
Otolith length (OL) (mm)	7.4913 ± 0.1	7.68819 ± 0.07	0.112
Otolith height (OH) (mm)	3.84127 ± 0.08	3.43848 ± 0.05	0.000 *
Area (mm ²)	20.62899 ± 0.74	20.26439 ± 0.35	0.619
Perimeters (mm)	19.62229 ± 0.38	19.4461 ± 0.18	0.636
OH/OL	0.51417 ± 0.01	0.44796 ± 0.01	0.000 *

Table 3. Cont.

Morphological Variables ⁺	Mean ± SE		p Value
	<i>Chelon auratus</i>	<i>Chelon saliens</i>	
Aspect ratio (OL/OH)	1.964 ± 0.04	2.2473 ± 0.03	0.000 *
Rectangularity (A/(OL × OH))	0.71783 ± 0.02	0.77017 ± 0.01	0.030 *
Compactness (P ² /A)	18.84561 ± 0.42	18.72685 ± 0.18	0.765
Otolith Shape indices—form factor = 4πA/p ²	0.67247 ± 0.01	0.67292 ± 0.01	0.973
Otolith Shape indices—roundness = 4A/(π(OL) ²)	0.46658 ± 0.01	0.437 ± 0.01	0.015 *
Otolith Shape indices—circularity(P ² /A)	18.84561 ± 0.42	18.72685 ± 0.18	0.765
ellipticity (E = (OL – OH/OL + OH))	0.32239 ± 0.01	0.38218 ± 0.01	0.000 *

⁺ Form factor provides an estimation for surface area irregularity, taking values of <1.0 when it was irregular and values of 1.0 when it was a perfect circle for the otolith shape index. The larger the value of the aspect ratio, the more elongated the otolith. Circularity and roundness illustrate the similarity of various features to a perfect circle, taking a minimum value of 1 and a maximum value of 4π. Rectangularity describes the variation in height and length with respect to the area, with 1.0 being a perfect square. Ellipticity indicates whether the changes in axis length are proportional.

Table 4. Characteristic loadings for PC1, PC2, and PC3, resulting from principal components analysis (PCA) of 13 morphometric characteristics of the otolith of *C. auratus* and *C. saliens*. Values in bold are significant.

Variable ⁺	Communalities		Component		
	Initial	Extraction	PC1	PC2	PC3
Otolith weight (OW) (g)	1	0.537	0.035	0.149	0.193
Otolith length (OL) (mm)	1	0.908	0.082	0.055	0.174
Otolith height (OH) (mm)	1	0.945	−0.168	0.146	0.118
Area (mm ²)	1	0.858	0.003	0.068	0.354
Perimeters (mm)	1	0.811	0.079	0.166	0.253
OH/OL	1	0.980	−0.199	0.111	−0.016
Aspect ratio	1	0.971	0.200	−0.102	0.004
Rectangularity	1	0.986	0.122	−0.126	0.188
Compactness	1	0.971	0.104	0.266	−0.105
Form factor	1	0.928	−0.098	−0.264	0.134
Roundness	1	0.988	−0.080	−0.015	0.216
Circularity	1	0.971	0.104	0.266	−0.105
Ellipticity	1	0.984	0.199	−0.113	0.014

⁺ The indices were calculated by the following equations: aspect ratio = OL/OH; rectangularity = A/(OL × OH); compactness = P²/A; otolith shape indices—form factor = 4πA/p²; otolith shape indices—roundness = 4A/(π(OL)²); otolith shape indices—circularity (P²/A); ellipticity (E = (OL – OH/OL + OH)).

The differences between *C. auratus* and *C. saliens* in the morphology of the otolith were significant (Wilk’s lambda = 0.46, χ² = 35.00, d.f. = 11, p < 0.05). The morphological characteristics of the otolith differences between the *C. auratus* and *C. saliens* of the south Caspian Sea can be successfully described using one function, discriminate function (DC1), which could explain 100% of the variation. According to the discriminative analysis output, 84.9% of pectoral fin spines were correctly classified, allowing for the separation of both species based on their otolith morphology. The cross-validated classification in the discriminate analysis indicated that 71.7% of all otoliths were assigned to the correct species. The dendrogram (Figure 5) grouped the two species into two major subgroups based on the analysis of significant otolith data. While *C. saliens* is observed in both subgroups, *C. auratus* was present only in one group. This illustrates that mullets already possess morphological traits linked to environmental factors, genetic differences, or a combination of these factors, which could be useful in completing identification keys.

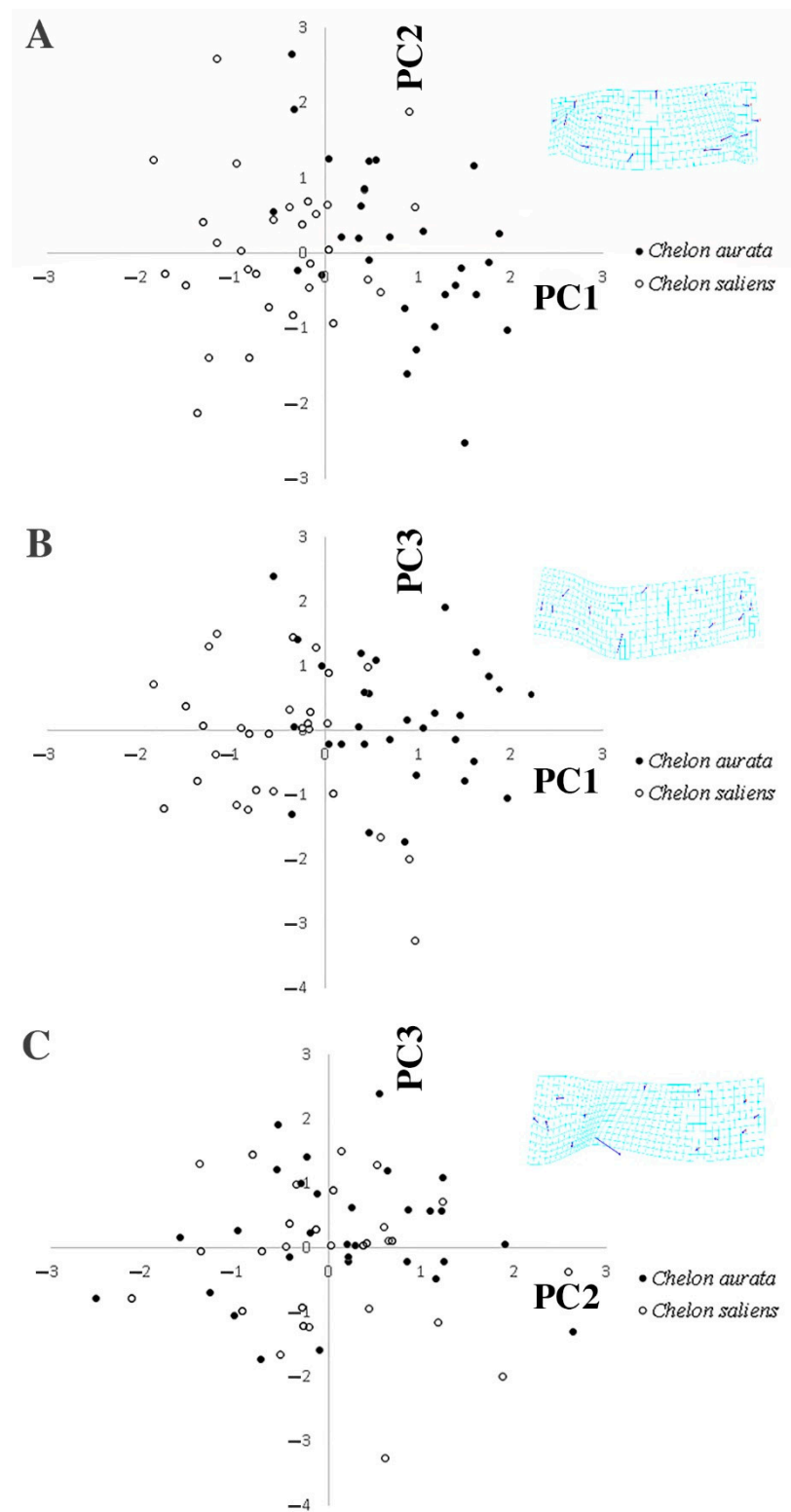


Figure 4. Principal component analysis (PCA) of the morphological variables of the body shapes of two mullet species (*C. saliens* and *C. auratus*). The scatter plot displays individual fish scores for PC1 vs. PC2 (A), PC1 vs. PC3 (B) and PC2 vs. PC3 (C), which together represent a total variance of 68%. Deformation grids (splines) are explained on the right side of each scatter plot. The splines represent fish shape variability along each relative PC axis.

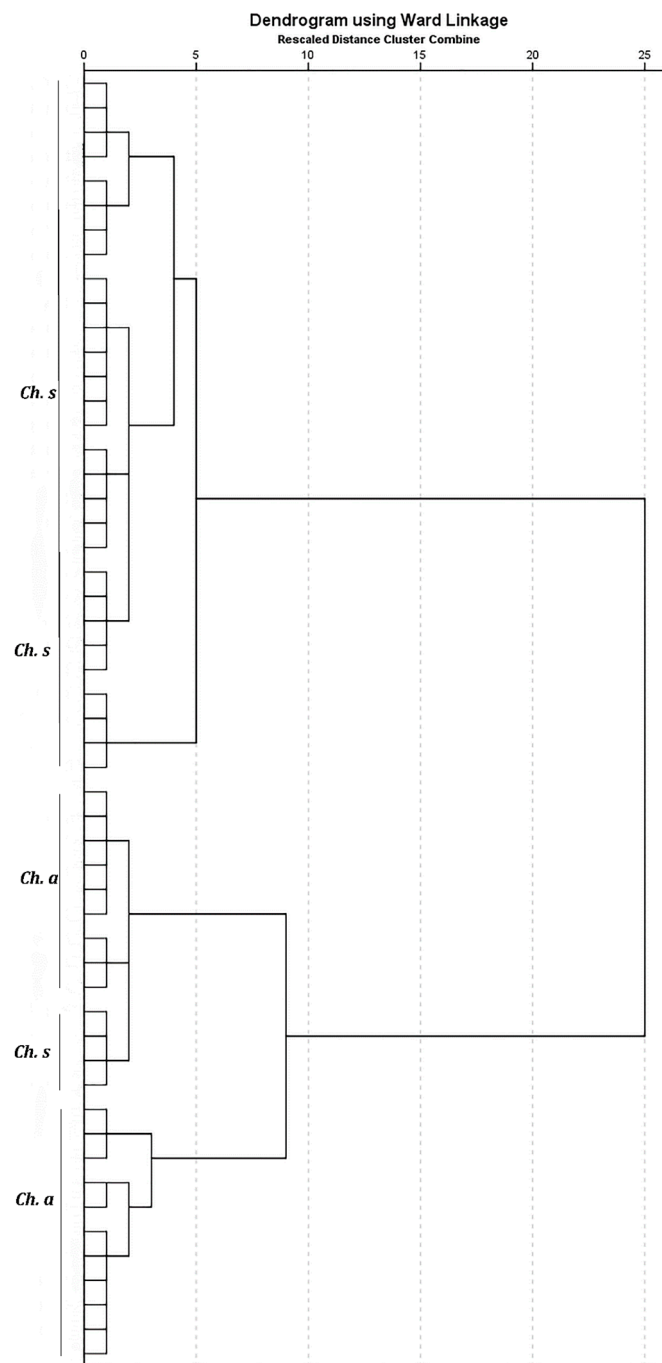


Figure 5. Dendrogram derived from cluster analysis for morphological variables of the otolith shape of the two mullet species (*C. saliens* and *C. auratus*). *Ch. s*: *Chelon saliens* individual otolith shape; *Ch. a*: *Chelon auratus* individual otolith shape.

4. Discussion

The assessment of the morphological differences between cryptic and very similar species is essential to better understand their variability in relation to habitats and environmental factors [42–44]. All methods of analysis showed morphological differences in body and otolith shapes between the two species. These differences were demonstrated by rectangulity, ellipticity, and the aspect ratio, as well as otolith height. Therefore, these species-specific traits can be used to distinguish these very similar species; moreover, they can be attributed to ecological differences and might represent the species’ adaptation to the distinct environmental characteristics of their habitat [31,38,40,45–51]. As such, divergence

in the otolith shapes of *C. auratus* and *C. saliens* might also be related to differences in habitat, behavior, preferred depth, and swimming activity. Although the link between otolith shape and certain ecological characteristics, such as depth and feeding behavior, is not well understood for temperate fish species, several studies have demonstrated a correlation between otoliths with rounded shapes and depth and feeding behaviors. Concerning the last point, for some fish species with rounded otoliths, it has been demonstrated that they mainly feed on organisms associated with the substrate, and this does not require a pronounced swimming performance [52–54]. Bani et al. [38], concluded that otolith shape is a good index for the correct identification of gobies, providing maximum distinction among species. In this study, aspect ratio, rectangularity, and ellipticity were greater in *C. saliens*, which live in pelagic water, compared to *C. auratus*. Significant differences in the aspect ratios of the otoliths between the mullet species reveal that the otoliths in *C. saliens* grow in length, while the otoliths of *C. auratus* mainly grow in thickness. The differences in the patterns of otolith growth were dependent on otolith thickness and mass, which is related to reliance on sounds and suitable reactions for predation; this usually increases with depth [38,55,56] and supports the pelagic habitat use of *C. saliens*. Although correlations between morphology and habitat have been found in several studies [47,57–64], morphological studies of wild populations do not sufficiently describe all of their adaptive responses to habitats and environmental conditions [62]. In vitro experiments are generally required, together with studies on otolith morphology. Furthermore, the comparison of the otoliths of different species and their populations are essential for improving our knowledge of these differences and our ability to detect them [1,47,57,65,66].

Evaluating these geometric morphometric parameters also confirms heterogeneity in the body traits of *C. auratus* and *C. saliens*, which could be interpreted as evidence of adaptive divergence. As body shape becomes more elongated in *C. auratus*, the snout becomes more pointed and the eyes are inclined downwards. The phenotypic traits are under the influence of natural selection and the composite effects of environmental factors such as temperature, depth strata preference, salinity, and trophic groups, in addition to genetic and ontogenetic factors [1,26,66–68]. Fish head and mouth morphology is usually associated with their feeding behaviors [58,59,61,62]. *Chelon saliens* was characterized by traits associated with fish in inshore areas, and also those that enter lagoons, rivers, and shallow habitats; these traits include large body depths, a robust head, and eyes inclined upwards [13]. However, adaptive traits are common patterns of mullet selection in natural conditions [13,25,68]. Mulletts are well known for their ability to feed on a quite wide variety of food items, allowing for the utilization of pelagic and benthic habitats over depths of 5–700m at salinities ranging from 4–13 ppt in the aquatic environment, with similar morphs in the same environments [13,20,68]. However, these species have shown different preferences in habitat usage and spawning time; furthermore, the selection of particle size in their diet could be a way to avoid competition [13,23,69].

Aside from divergence in food resources, the habitats of the two species also differ with regard to their thermal conditions, which cause pelagic habitats to undergo large seasonal changes in water temperature between the warm summer months and the cold winter months [13,19,20,68]. Moreover, the divergence of the morphs in the habitat may be related to alternative strategies for surviving in an environment with low temperatures. This leads to fish of smaller sizes, similar to *C. saliens* [13,69]. Moreover, the wider and shorter caudal peduncle, smaller head, and smaller snout of *C. saliens* in comparison to *C. auratus* coincides with previous traditional morphometric research [13,20,67,70].

On the other hand, discriminate analysis indicates that *C. auratus* and *C. saliens* are shaped uniquely, and the differences found may reflect the taxonomic distinctiveness of the species.

The present study confirmed the presence of variability in the shape and morphological characteristics of sagittae between species from a similar geographical region. These species have high economic and ecological importance [1,71], meaning that it is crucial to have an understanding of their abundance, demographic history, and genetic connectivity,

especially for very similar species, such as *C. auratus* and *C. saliens*, which are greatly exploited in the south Caspian Sea. The identification of Mugilidae is very important for commercial purposes, the management of fisheries, and regulation [47,68]. Although the morphological characters of different species of *Chelon* vary, it is difficult to identify them using general morphology only [68]. Our findings indicate that external morphology and otolith shape are adequately distinct to allow the discrimination of the two Caspian Sea mullets based on discriminant function and morphometric indices. These differences can be applied to the prediction of preferred habitats and differences in local adaptation [72–74].

Author Contributions: Conceptualization, S.B. and F.T.; methodology, S.B., F.T., K.A., A.R.L., A.B. and A.P.; validation, S.B. and F.T.; data curation, S.B.; writing—original draft preparation, S.B., F.T., K.A., A.R.L., A.B. and A.P.; writing—review and editing, F.T. and S.B. All authors have read and agreed to the published version of the manuscript.

Funding: The University of Guilan, Iran supported this research (with the reference Grant No. 2772811-1398.3.27).

Acknowledgments: The University of Guilan, Iran supported this research (with the reference Grant No. 2772811-1398.3.27). We would like to thank Guilan University sectors including the Director of International Scientific Cooperation Office and the Vice Chancellor of Research, as well as the Inland Waters Aquaculture Research Center. We also thank the Iranian Fisheries Sciences Research Institute for their assistance.

Conflicts of Interest: The authors declare that they have no personal relationships that could have influenced the research reported in this study; nor do they have any competing financial interest.

References

1. D'iglio, C.; Natale, S.; Albano, M.; Savoca, S.; Famulari, S.; Gervasi, C.; Lanteri, G.; Panarello, G.; Spanò, N.; Capillo, G. Otolith Analyses Highlight Morpho-Functional Differences of Three Species of Mullet (Mugilidae) from Transitional Water. *Sustainability* **2022**, *14*, 398. [CrossRef]
2. Elgueta, A.; Thoms, M.C.; Górski, K.; Díaz, G.; Habit, E.M. Functional process zones and their fish communities in temperate Andean river networks. *River Res. Appl.* **2019**, *35*, 1702–1711. [CrossRef]
3. Kelley, J.L.; Grierson, P.F.; Collin, S.P.; Davies, P.M. Habitat disruption and the identification and management of functional trait changes. *Fish Fish.* **2018**, *19*, 716–728. [CrossRef]
4. Weiskopf, S.R.; Rubenstein, M.A.; Crozier, L.G.; Gaichas, S.; Griffis, R.; Halofsky, J.E.; Hyde, K.J.W.; Morelli, T.L.; Morissette, J.T.; Muñoz, R.C.; et al. Climate change effects on biodiversity, ecosystems, ecosystem services, and natural resource management in the United States. *Sci. Total Environ.* **2020**, *733*, 137782. [CrossRef]
5. Mattone, C.; Bradley, M.; Barnett, A.; Konovalov, D.A.; Sheaves, M. Environmental conditions constrain nursery habitat value in Australian sub-tropical estuaries. *Mar. Environ. Res.* **2022**, *175*, 105568. [CrossRef]
6. Michaud, B.C.; Kilborn, J.P.; MacDonald, T.C.; Peebles, E.B. A description of Florida estuarine gradient complexes and the implications of habitat factor covariation for community habitat analysis. *Estuar. Coast. Shelf Sci.* **2022**, *264*, 107669. [CrossRef]
7. Arai, T. Migration ecology in the freshwater eels of the genus *Anguilla* Schrank, 1798. *Trop. Ecol.* **2022**, *63*, 155–170. [CrossRef]
8. Bakhshalizadeh, S.; Bani, A. Morphological analysis of pectoral fin spine for identifying ecophenotypic variation of Persian Sturgeon *Acipenser persicus*. *Mar. Ecol.* **2018**, *39*, e12516. [CrossRef]
9. DeWitt, T.J.; Troendle, N.J.; Mateos, M.; Mauricio, R. Population genetics and independently replicated evolution of predator-associated burst speed ecophenotypy in mosquitofish. *Heredity* **2022**, *128*, 45–55. [CrossRef]
10. Proćków, M.; Proćków, J.; Błazej, P.; Mackiewicz, P. The influence of habitat preferences on shell morphology in ecophenotypes of *Trochulus hispidus* complex. *Sci. Total Environ.* **2018**, *630*, 1036–1043. [CrossRef]
11. Smith, S.R.; Amish, S.J.; Bernatchez, L.; le Luyer, J.; Wilson, C.; Boeberitz, O.; Luikart, G.; Scribner, K.T. Mapping of Adaptive Traits Enabled by a High-Density Linkage Map for Lake Trout. *Genes Genomes Genet.* **2020**, *10*, 1929–1947. [CrossRef]
12. Cerda, J.M.; Palacios-Fuentes, P.; Díaz-Santana-Iturrios, M.; Ojeda, F.P. Description and discrimination of sagittae otoliths of two sympatric labrisomid blennies *Auchenionchus crinitus* and *Auchenionchus microcirrhis* using morphometric analyses. *J. Sea Res.* **2021**, *173*, 102063. [CrossRef]
13. Coad, B.W. Review of the freshwater mullets of Iran (family mugilidae). *Iran. J. Ichthyol.* **2017**, *4*, 75–130. [CrossRef]
14. Gallien, L.; Carboni, M. The community ecology of invasive species: Where are we and what's next? *Ecography* **2017**, *40*, 335–352. [CrossRef]
15. Latorre Espeso, D. Effects of Environmental Conditions on Phenotypic Plasticity of Fishes in Iberian Waters: Life-History, Physiological and Morphological Traits. Ph.D. Thesis, Universitat de Girona, Girona, Spain, 2019.
16. Ren, P.; He, H.; Song, Y.; Cheng, F.; Xie, S. The spatial pattern of larval fish assemblages in the lower reach of the Yangtze River: Potential influences of river–lake connectivity and tidal intrusion. *Hydrobiologia* **2016**, *766*, 365–379. [CrossRef]

17. Bakhshalizadeh, S.; Abbasi, K.; Rostamzade Liafuie, A.; Nezamdoost Darestani, R. *A Guideline on the Identification of Economical Fish of the South Caspian Sea*; Jahad Daneshgahi University: Teheran, Iran, 2021.
18. Barati, A. Diet and growth of chicks of the Great Cormorant, *Phalacrocorax carbo*, at Ramsar, northern Iran. (Aves: Phalacrocoraciidae). *Zool. Middle East* **2009**, *46*, 29–36. [[CrossRef](#)]
19. Fazli, H.; Ghaninejad, D.; Janbaz, A.A.; Daryanabard, R. Population ecology parameters and biomass of golden grey mullet (*Liza aurata*) in Iranian waters of the Caspian Sea. *Fish. Res.* **2008**, *93*, 222–228. [[CrossRef](#)]
20. Pourfaraj, V.; Karami, M.; Nezami, S.; Rafiee, G.; Khara, H. Morphological variation of Golden mullet, *Liza aurata*, of southern coasts of the Caspian Sea. *Iran. Sci. Fish. J.* **2008**, *17*, 35–48.
21. Cardona, L. Selección del hábitat por los mugílidos (*Osteichthyes: Mugilidae*) en los estuarios mediterráneos: El papel de la salinidad. *Sci. Mar.* **2007**, *70*, 443–455. [[CrossRef](#)]
22. Froese, R.; Pauly, D. FishBase. 2022. Available online: www.fishbase.org. (accessed on 13 September 2022).
23. Kesiktaş, M.; Yemişken, E.; Yildiz, T.; Eryilmaz, L. Age, growth and reproduction of the golden grey mullet, *Chelon auratus* (Risso, 1810) in the Golden Horn Estuary, Istanbul. *J. Mar. Biol. Assoc. UK* **2020**, *100*, 989–995. [[CrossRef](#)]
24. Katselis, G.; Hotos, G.; Minos, G.; Vidalis, V. Phenotypic affinities on fry of four Mediterranean grey mullet species. *Turk. J. Fish. Aquat. Sci.* **2006**, *6*, 49–55.
25. Quattrocchi, F.; D’Anna, G.; Fiorentino, F.; Titone, A.; Zenone, A.; Garofalo, G. Phenotypic variation across populations of red mullet (*Mullus barbatus*) in different environments of the central Mediterranean. *Mar. Freshw. Res.* **2020**, *71*, 1313–1326. [[CrossRef](#)]
26. Cadrin, S.X. Advances in morphometric identification of fishery stocks. *Rev. Fish Biol. Fish.* **2000**, *10*, 91–112. [[CrossRef](#)]
27. Pazzaglia, J.; Reusch, T.B.H.; Terlizzi, A.; Marín-Guirao, L.; Procaccini, G. Phenotypic plasticity under rapid global changes: The intrinsic force for future seagrasses survival. *Evol. Appl.* **2021**, *14*, 1181–1201. [[CrossRef](#)]
28. Xue, B.K.; Leibler, S. Benefits of phenotypic plasticity for population growth in varying environments. *Proc. Natl. Acad. Sci. USA* **2018**, *115*, 12745–12750. [[CrossRef](#)]
29. Azzurro, E.; Tuset, V.M.; Lombarte, A.; Maynou, F.; Simberloff, D.; Rodríguez-Pérez, A.; Solé, R.V. External morphology explains the success of biological invasions. *Ecol. Lett.* **2014**, *17*, 1455–1463. [[CrossRef](#)]
30. Smith, S.M.; Fox, R.J.; Donelson, J.M.; Head, M.L.; Booth, D.J. Predicting range-shift success potential for tropical marine fishes using external morphology. *Biol. Lett.* **2016**, *12*, 3–7. [[CrossRef](#)]
31. Ugrin, N.; Škeljo, F.; Ferri, J.; Krstulović Šifner, S. Use of otolith morphology and morphometry for species discrimination of megrims *Lepidorhombus* spp. in the Central Eastern Adriatic Sea. *J. Mar. Biol. Assoc. UK* **2021**, *101*, 735–741. [[CrossRef](#)]
32. Helland, I.P.; Vøllestad, L.A.; Freyhof, J.; Mehner, T. Morphological differences between two ecologically similar sympatric fishes. *J. Fish Biol.* **2006**, *75*, 2756–2767. [[CrossRef](#)]
33. Valentin, A.E.; Penin, X.; Chanut, J.-P.; Sévigny, J.-M.; Rohlf, F.J. Arching effect on fish body shape in geometric morphometric studies. *J. Fish Biol.* **2008**, *73*, 623–638. [[CrossRef](#)]
34. Zelditch, M.L.; Swiderski, D.L.; Sheets, H.D. Introduction. *Geom. Morphometrics Biol.* **2012**, *95*, 1–20. [[CrossRef](#)]
35. Franssen, N.R. Anthropogenic habitat alteration induces rapid morphological divergence in a native stream fish. *Evol. Appl.* **2011**, *4*, 791–804. [[CrossRef](#)]
36. Khan, M.A.; Nazir, A. Stock delineation of the long-whiskered catfish, *Sperata aor* (Hamilton 1822), from River Ganga by using morphometrics. *Mar. Freshw. Res.* **2018**, *70*, 107–113. [[CrossRef](#)]
37. Tuset, V.M.; Lombarte, A.; Assis, C.A. Otolith atlas for the western Mediterranean, north and central eastern Atlantic. *Sci. Mar.* **2008**, *72*, 7–198. [[CrossRef](#)]
38. Bani, A.; Poursaeid, S.; Tuset, V.M. Comparative morphology of the sagittal otolith in three species of south Caspian gobies. *J. Fish Biol.* **2013**, *82*, 1321–1332. [[CrossRef](#)]
39. Lombarte, A.; Gordo, A.; Whitfield, A.K.; James, N.C.; Tuset, V.M. Ecomorphological analysis as a complementary tool to detect changes in fish communities following major perturbations in two South African estuarine systems. *Environ. Biol. Fishes* **2012**, *94*, 601–614. [[CrossRef](#)]
40. Lombarte, A.; Lleonart, J. Otolith size changes related with body growth, habitat depth and temperature. *Environ. Biol. Fishes* **1993**, *37*, 297–306. [[CrossRef](#)]
41. Quinn, G.; Keough, M. *Experimental Design and Data Analysis for Biologists*; Cambridge University Press: Cambridge, UK, 2002. [[CrossRef](#)]
42. Chenuil, A.; Cahill, A.E.; Délémontey, N.; Salliant du Luc, E.D.; Fanton, H. Problems and questions posed by cryptic species. A framework to guide future studies. In *From Assessing to Conserving Biodiversity*; Springer: Cham, Switzerland, 2019; pp. 77–106.
43. Fi, C.; Robinson, C.T.; Malard, F. Cryptic species as a window into the paradigm shift of the species concept. *Mol. Ecol.* **2018**, *27*, 613–635. [[CrossRef](#)]
44. Naciri, Y.; Linder, H.P. Species delimitation and relationships: The dance of the seven veils. *Taxon* **2015**, *64*, 3–16. [[CrossRef](#)]
45. Assis, C.A. The utricular otoliths, lapilli, of teleosts: Their morphology and relevance for species identification and systematics studies. *Sci. Mar.* **2005**, *69*, 259–273. [[CrossRef](#)]
46. Assis, I.O.; da Silva, V.E.L.; Souto-Vieira, D.; Lozano, A.P.; Volpedo, A.V.; Fabrè, N.N. Ecomorphological patterns in otoliths of tropical fishes: Assessing trophic groups and depth strata preference by shape. *Environ. Biol. Fishes* **2020**, *103*, 349–361. [[CrossRef](#)]
47. Callicó Fortunato, R.; Benedito Durà, V.; Volpedo, A. The morphology of saccular otoliths as a tool to identify different mugilid species from the Northeastern Atlantic and Mediterranean Sea. *Estuar. Coast. Shelf Sci.* **2014**, *146*, 95–101. [[CrossRef](#)]

48. He, T.; Chen, C.J.; Qin, J.G.; Li, Y.; Wu, R.H.; Gao, T.X. The use of otolith shape to identify stocks of redlip mullet, *Liza haematocheilus*. *Pak. J. Zool.* **2020**, *52*, 2265–2273. [[CrossRef](#)]
49. Nazir, A.; Khan, M.A. Using otoliths for fish stock discrimination: Status and challenges. *Acta Ichthyol. Piscat.* **2021**, *51*, 199–218. [[CrossRef](#)]
50. Radhakrishnan, K.V.; Li, Y.; Jayalakshmy, K.V.; Liu, M.; Murphy, B.R.; Xie, S. Application of otolith shape analysis in identifying different ecotypes of *Coilia ectenes* in the Yangtze Basin, China. *Fish. Res.* **2012**, *125*, 156–160. [[CrossRef](#)]
51. SriHari, M.; Bhushan, S.; Nayak, B.B.; Pavan-Kumar, A.; Abidi, Z.J. Spatial Variations in the Stocks of Randall's Threadfin Bream, *Nemipterus randalli* Russell 1986 Along the Indian Coast Inferred Using Body and Otolith Shape Analysis. *Thalassas* **2021**, *37*, 883–890. [[CrossRef](#)]
52. Gagliano, M.; McCormick, M.I. Feeding history influences otolith shape in tropical fish. *Mar. Ecol. Prog. Ser.* **2004**, *278*, 291–296. [[CrossRef](#)]
53. Mille, T.; Mahé, K.; Cachera, M.; Villanueva, M.C.; de Pontual, H.; Ernande, B. Diet is correlated with otolith shape in marine fish. *Mar. Ecol. Prog. Ser.* **2016**, *555*, 167–184. [[CrossRef](#)]
54. Volpedo, A.; Echeverr, D.D. Ecomorphological patterns of the sagitta in fish on the continental shelf off Argentina. *Fish. Res.* **2003**, *60*, 551–560. [[CrossRef](#)]
55. Gauldie, R.W.; Crampton, J.S. An eco-morphological explanation of individual variability in the shape of the fish otolith: Comparison of the otolith of *Hoplostethus atlanticus* with other species by depth. *J. Fish Biol.* **2002**, *60*, 1204–1221. [[CrossRef](#)]
56. Libungan, L.A.; Óskarsson, G.J.; Slotte, A.; Jacobsen, J.A.; Pálsson, S. Otolith shape: A population marker for Atlantic herring *Clupea harengus*. *J. Fish Biol.* **2015**, *86*, 1377–1395. [[CrossRef](#)]
57. Callicó Fortunato, R.; González-Castro, M.; Reguera Galán, A.; García Alonso, I.; Kunert, C.; Benedito Durà, V.; Volpedo, A. Identification of potential fish stocks and lifetime movement patterns of *Mugil liza* Valenciennes 1836 in the Southwestern Atlantic Ocean. *Fish. Res.* **2017**, *193*, 164–172. [[CrossRef](#)]
58. Conith, A.J.; Kidd, M.R.; Kocher, T.D.; Albertson, R.C. Ecomorphological divergence and habitat lability in the context of robust patterns of modularity in the cichlid feeding apparatus. *BMC Evol. Biol.* **2020**, *20*, 95. [[CrossRef](#)] [[PubMed](#)]
59. Costeur, L.; Grohé, C.; Aguirre-Fernández, G.; Ekdale, E.; Schulz, G.; Müller, B.; Mennecart, B. The bony labyrinth of toothed whales reflects both phylogeny and habitat preferences. *Sci. Rep.* **2018**, *8*, 8–13. [[CrossRef](#)]
60. Pasingi, N.; Olii, A.H.; Habibie, S.A. Morphology and growth pattern of Nike fish (amphidromous goby larvae) in Gorontalo Waters, Indonesia. Tomini. *J. Aquat. Sci.* **2020**, *1*, 1–7. [[CrossRef](#)]
61. Schrandt, M.N.; Switzer, T.S.; Stafford, C.J.; Flaherty-Walia, K.E.; Paperno, R.; Matheson, R.E. Similar habitats, different communities: Fish and large invertebrate assemblages in eastern Gulf of Mexico polyhaline seagrasses relate more to estuary morphology than latitude. *Estuar. Coast. Shelf Sci.* **2018**, *213*, 217–229. [[CrossRef](#)]
62. Torres-Dowdall, J.; Handelsman, C.A.; Reznick, D.N.; Ghalambor, C.K. Local Adaptation and the Evolution of Phenotypic Plasticity in Trinidadian Guppies (*Poecilia reticulata*). *Evolution* **2012**, *66*, 3432–3443. [[CrossRef](#)]
63. Wegscheider, B.; Linnansaari, T.; Curry, R.A. Mesohabitat modelling in fish ecology: A global synthesis. *Fish Fish.* **2020**, *21*, 927–939. [[CrossRef](#)]
64. Yedier, S.; Bostanci, D. Aberrant otoliths in four marine fishes from the Aegean Sea, Black Sea, and Sea of Marmara (Turkey). *Reg. Stud. Mar. Sci.* **2020**, *34*, 101011. [[CrossRef](#)]
65. Clark, F.J.K.; da Silva Lima, C.S.; Pessanha, A.L.M. Otolith shape analysis of the Brazilian silverside in two northeastern Brazilian estuaries with distinct salinity ranges. *Fish. Res.* **2021**, *243*, 106094. [[CrossRef](#)]
66. D'Iglio, C.; Albano, M.; Famulari, S.; Savoca, S.; Panarello, G.; di Paola, D.; Perdichizzi, A.; Rinelli, P.; Lanteri, G.; Spanò, N.; et al. Intra- and interspecific variability among congeneric *Pagellus otoliths*. *Sci. Rep.* **2021**, *11*, 16315. [[CrossRef](#)]
67. Khayyami, H.; Movahedinia, A.; Zolgharnein, H.; Salamat, N. Morphological variability of *Liza aurata* (Risso, 1810), along the southern Caspian Sea. *J. Basic Appl. Zool.* **2014**, *67*, 100–107. [[CrossRef](#)]
68. Whitfield, A.K.; Panfili, J.; Durand, J.-D. A global review of the cosmopolitan flathead mullet *Mugil cephalus* Linnaeus 1758 (*Teleostei: Mugilidae*), with emphasis on the biology, genetics, ecology and fisheries aspects of this apparent species complex. *Rev. Fish Biol. Fish.* **2012**, *22*, 641–681. [[CrossRef](#)]
69. Ghaninejad, D. Maturity Stages, Gonado-Somatic Index (GSI) and Fecundity of Leaping Grey Mullet, *Liza saliens* (Risso, 1810) in the Western Part of Iranian Waters of the Caspian Sea (Guilan Province, Iran). *Asian Fish. Sci.* **2011**, *24*, 115–124. [[CrossRef](#)]
70. Ghaninejad, D.; Parafkandeh Haghighi, F.; Abdolmaleki, S.; Nahrevar, R.; Khedmati, K.; Rastin, R.; Nikpour, M. Morphometric and Meristic Characteristics of *Liza aurata* Risso 1810 in the South of Caspian Sea. *New Technol. Aquac. Dev. J. Fish.* **2012**, *6*, 31–42.
71. Qiao, J.; Zhu, R.; Chen, K.; Zhang, D.; Yan, Y.; He, D. Comparative Otolith Morphology of Two Morphs of *Schizopygopsis thermalis* Herzenstein 1891 (Pisces, Cyprinidae) in a Headwater Lake on the Qinghai-Tibet Plateau. *Fishes* **2022**, *7*, 99. [[CrossRef](#)]
72. Bakhshalizadeh, S.; Bani, A. Uso de morfometría geométrica para la identificación de variaciones ecofenotípicas en juveniles de esturión persa *acipenser persicus*. *Sci. Mar.* **2017**, *81*, 187–193. [[CrossRef](#)]
73. Bostanci, D.; Yedier, S. Discrimination of invasive fish *Atherina boyeri* (Pisces: Atherinidae) populations by evaluating the performance of otolith morphometrics in several lentic habitats. *Fresenius Environ. Bull.* **2018**, *27*, 4493–4501.
74. Terada, C.; Saitoh, T. Phenotypic and genetic divergence among island populations of sika deer (*Cervus nippon*) in southern Japan: A test of the local adaptation hypothesis. *Popul. Ecol.* **2018**, *60*, 211–221. [[CrossRef](#)]